APPLICATION OF TWO-DIMENSIONAL MATCHED FILTERS TO X-RAY RADIOGRAPHIC FLAW DETECTION AND ENHANCEMENT

R.M. Wallingford, E.M. Siwek and J.N.Gray

Center for Nondestructive Evaluation and the
FAA Center for Aviation Systems Reliability
Iowa State University, Ames, IA 50011

INTRODUCTION

Detection and enhancement of low contrast flaws in radiographic images with high noise fields is an ongoing topic of research in nondestructive evaluation. In film radiography, the minimum detectable flaw thickness is controlled by the exposure characteristics and the flaw size in relation to the thickness of the part. The exposure characteristics determine the overall sensitivity and noise level, while the flaw thickness controls the contrast of the flaw image with respect to the background film density. Often it is difficult to generate optimal exposures when inspecting thick objects or complicated part geometries. This can result in noisy images due to the poor counting statistics of the photons as well as optical film densities that are suboptimal for visual interpretation. In addition, flaw contrast is often extremely low due to the flaw size or the poor orientation of crack-like flaws. The goal of the work presented in this paper is to demonstrate the utility of digital image processing using the matched filter for detecting and enhancing flaws in low-contrast, high-noise radiographic images. The basic theory of the matched filter will be presented along with its application to two-dimensional images, In addition several practical examples will be shown on simulated and real radiographs.

MATCHED FILTER BACKGROUND AND THEORY

Matched filtering is a powerful technique for detecting signals in which the signal function is known a priori. It originated in 1943 in pulsed radar detection [1] and has recently been extended to two-dimensions and applied to images in blood vessel detection, cloud clutter suppression and fingerprint enhancement [2-4]. It is essentially a cross-correlation filter in which the correlation functions are the measured noisy signal or image and the expected ideal signal. The one-dimensional matched filter is given by Eq. (1)

$$g(m) = \sum_{i=1}^{M} f(i+m)h(i) \tag{1}$$

where $f(i)$ is the measured noisy signal and $h(i)$ is the expected signal to be detected.

This filter can be generalized to the two-dimensional image and is given by

Review of Progress in Quantitative Nondestructive Evaluation, Vol. 11
Edited by D.O. Thompson and D.E. Chimenti, Plenum Press, New York, 1992

$$g(m,n) = \sum_{i=1}^{M} \sum_{j=1}^{N} f(i+m, j+n)h(i, j) \tag{2}$$

where $f(i, j)$ is the measured image function, $h(i, j)$ is a template containing the ideal expected signal or flaw function, and (M, N) is the size of the template, h.

In both the one and two-dimensional cases, the filters can equivalently be represented as convolutions for simple implementation in the frequency domain. However, we choose to use the correlation implementation since image processing hardware and software is readily available for fast template correlation.

In the case of an image corrupted by additive white noise, the filter function, h, which contains the expected flaw signal can be shown to maximize the signal-to-noise ratio. Consider the general linear filter equation

$$f_o(m,n) = \{ f_i(m,n) + n_i(m,n)\} * h(m,n) \tag{3}$$

where the image function consists of the ideal signal $f_i(m,n)$ with an additive noise term, $n_i(m,n)$. We can express the energy in the image due to the signal alone as

$$|S(m,n)|^2 = |f_i(m,n) * h(m,n)|^2 \tag{4}$$

$$= \left| \mathcal{F}^{-1}\{F_i(\omega_x,\omega_y)H(\omega_x,\omega_y)\} \right|^2 , \tag{5}$$

and the energy in the image due to the white noise as

$$N = \frac{N_o}{2} \int \int |H(\omega_x,\omega_y)|^2 \, d\omega_x d\omega_y . \tag{6}$$

The signal-to-noise ratio is given by

$$\frac{|S(m,n)|^2}{N} = \frac{\left| \int \int F_i(\omega_x,\omega_y) H(\omega_x,\omega_y) \, exp\{i(\omega_x m + \omega_y n)\} \, d\omega_x d\omega_y \right|^2}{\frac{N_o}{2} \int \int |H(\omega_x,\omega_y)|^2 d\omega_x d\omega_y} . \tag{7}$$

It can be shown [5,6] that maximizing Eq. (7) with respect to the filter function, H, results in

$$h(i, j) = \frac{2}{N_o} f(m-i, n-j) . \tag{8}$$

Thus, the optimal convolution template is given by a shifted and reversed version of the ideal signal, f. The shifting of the signal implies that a maximum signal-to-noise ratio is obtained when the template is shifted to the signal location in the image. Note that for correlation implementation, the optimal filter function is simply a shifted version of the ideal signal, f.

Radiographic images are typically corrupted by a combination of colored film grain noise and signal dependent Poisson counting noise [7]. Thus, when using a filter template defined by Eq. (8) the resulting S/N will not be maximized. This is not of extreme concern, however, because in most cases the S/N is additionally degraded due to the inexact signal or flaw modeling. Although the optimal filter could be derived through

knowledge of the non-white noise spectrum using a pre-whitening filter [7], we have chosen not to implement it in this preliminary study.

Matched filtering is ideally suited for application to radiographic nondestructive testing because of the recent availability of radiographic inspection models [8] in which a priori information from a CAD model of the part can be incorporated into the filter. In addition, the expected overall flaw morphology is often known ahead of time. The radiographic inspection model can be used to generate more optimal filter elements which would otherwise suffer from background mismatch. Use of matched filters on images generated by the radiographic inspection models can also yield insight into bounds on minimum detectable flaw size for a given inspection. In the case of crack detection, which is highly orientation dependent, banks of matched filters can be used for detection of the crack location and orientation.

PRACTICAL EXAMPLES

Matched filters have been implemented and evaluated on a variety of real and simulated radiographic images. The simulated images consist of models of small spherical voids in a flat plate geometry of varying thickness and a spherical void in a simulated complex shape casting.

Figures 1-3 show the original flat-plate images with their corresponding results after matched filtering. The original images were generated using the x-ray simulation model of Gray et al. [9] and have flaw signal-to-noise ratios of 4.1 dB, -4.4 dB and -10 dB, respectively. The signal-to-noise ratios of the filtered images are 30 dB, 20 dB and 19 dB, respectively. The filter element used in this example was an 11x11 pixel circular hemisphere with a peak value of 1.0. Although this filter element is not optimal for maximum signal-to-noise improvement, it represents an acceptable compromise between performance, ease of implementation and an incomplete knowledge of the flaw morphology. The exact predicted filter shape could be computed, however, from the simulation model by artificially suppressing the noise. The pre-whitening filter could also be determined from the noise process of the model.

Notice that the original flaw signals in Figs. 2 and 3 are not visible to the eye, however, the filtered images readily reveal the flaw. Also notice the distorted flaw shape as well as the obvious texture in the filtered images. These characteristics are artifacts of the filtering and are currently under further investigation.

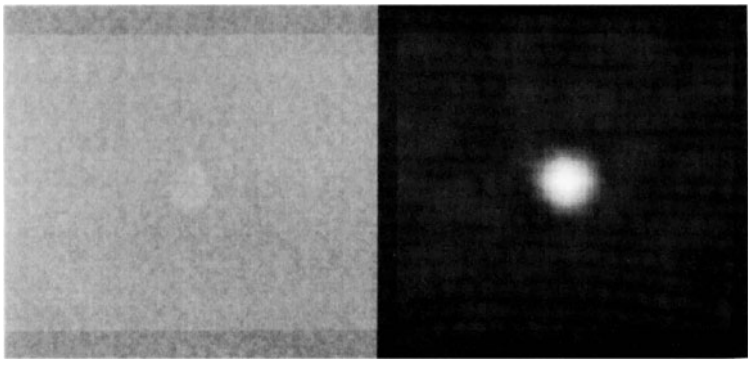

Figure 1. Simulated radiograph of a spherical flaw in a flat plate geometry and filtered result. Original S/N = 4.1 dB; Filtered S/N = 30 dB.

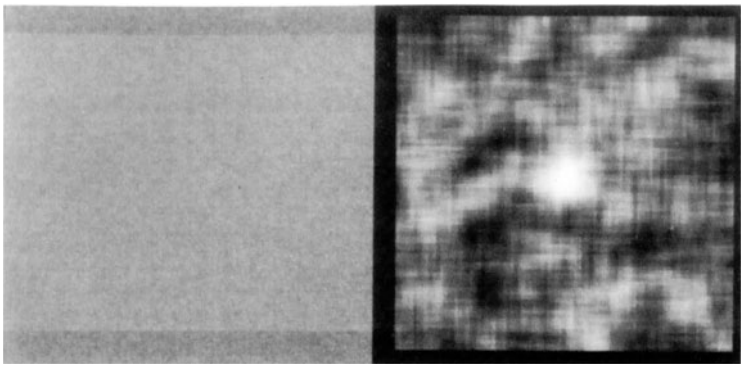

Figure 2. Simulated radiograph of a spherical flaw in a flat plate geometry and filtered result. Original S/N = -4.4 dB; Filtered S/N = 20 dB.

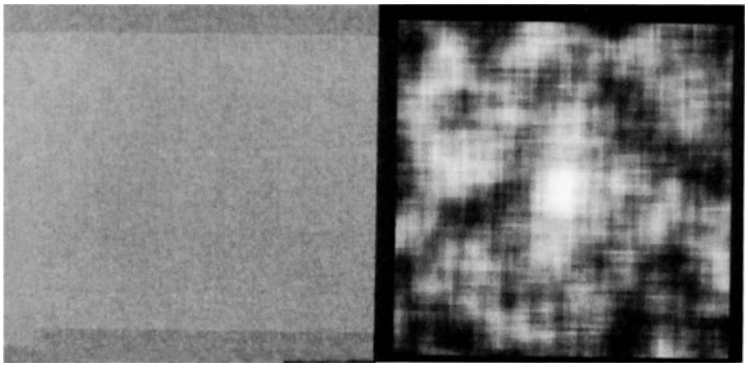

Figure 3. Simulated radiograph of a spherical flaw in a flat plate geometry and filtered result. Original S/N = -10 dB; Filtered S/N = 19 dB.

Matched filtering is also ideally suited for application to part geometries in which the background can either be modeled through a CAD description of the part in conjunction with the x-ray simulation model or removed entirely. In the former case, the background geometry is modeled as a component of the signal with the expected flaw signal superimposed. For situations where the general flaw location is unknown, this procedure works well only for regions in which the geometrical background variation is relatively constant. In other cases, the background for the filter element can be adaptively modeled using the x-ray simulation model.

The above procedure was applied to a simulated radiograph of an automobile air conditioner part shown in Figure 4a. The radiograph was generated using a CAD representation of the object and the x-ray simulation model. The object contains a spherical flaw along the outer right-hand edge of the part. The simulation model was also used to generate the matched filter template, consisting of a background trend with a superimposed hemispherical function. The elements of the filter template are given by

$$h = \begin{bmatrix} 29 & 23 & 18 & 11 & 5 \\ 26 & 20 & 15 & 8 & 3 \\ 25 & 19 & 13 & 7 & 1 \\ 24 & 18 & 13 & 6 & 0 \\ 25 & 19 & 14 & 7 & 1 \end{bmatrix}. \tag{9}$$

The resultant image after filtering is shown in Figure 4b. The signal-to-noise improvement for this case was 10 dB.

The matched filter has also been applied to real high-noise, low-contrast radiographic images. Figure 5a shows a digitized radiograph of 3 adjacent void-like flaws in an aluminum weld. In this case, the true flaw shape and intensity is not known a priori. However, we have found that a general normalized hemispherical function works well for a wide variety of area-type flaws when its diameter is less than the overall length of the flaw but is large enough for a correlation length sufficient to build up a good signal-to-noise ratio.

The result of the matched filter using a 13x13 circular hemispherical filter element is shown in Figure 5b. The estimated S/N of the flaws in the original image from top to bottom are 5.6 dB, 2.9 dB and 0.8 dB. The corresponding estimated flaw S/N for the filtered image are 19 dB, 13 dB and 13 dB, respectively. Even with a suboptimal filter function, these results show a significant improvement over the original image. A thresholded version of the filtered image is shown in Figure 6. Notice that each of the three flaws is now easily detectable.

Figure 7a shows a radiograph of a crack-like flaw in an aluminum weld. These types of flaws are easier to model and detect using matched filters since banks of filters can be used to estimate the crack orientation and the filter size can be reduced to simulate a piecewise linear crack shape. A tradeoff in this situation is that the correlation length is often too short to obtain significant improvement in S/N. In the example shown here, however, the crack is very straight and has sufficient width for a good correlation length. Thus, the filter element can be chosen to be relatively large. Figure 7b shows the filtered result using a two-dimensional horizontally invariant Gaussian with a 3σ width of 2 pixels. The original estimated S/N was 3.5 dB and the filtered S/N was 17 dB.

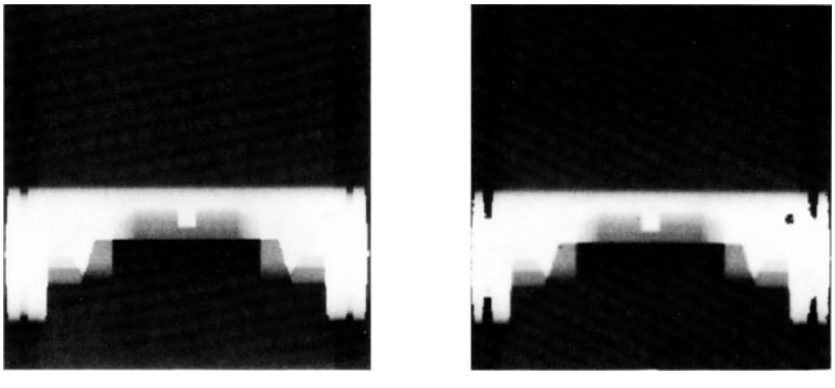

(a) (b)

Figure 4. a) Original simulated radiograph of a complex casting part.
b) Filtered result.

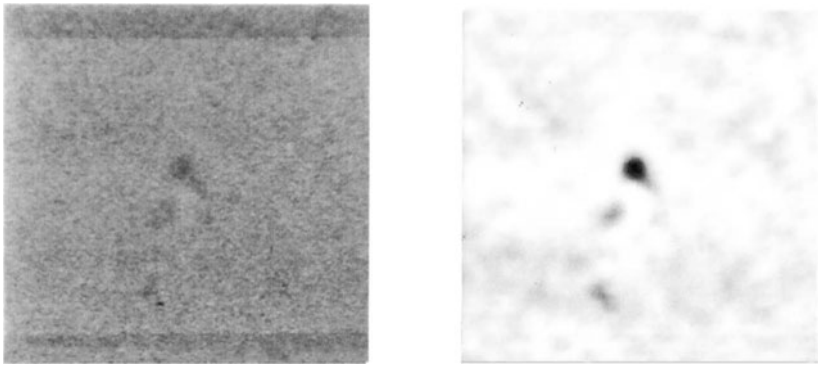

(a) (b)

Figure 5. a) Original radiograph of void-like flaws in an aluminum weld.
b) Filtered result.

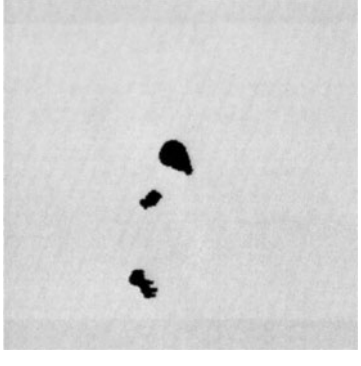

Figure 6. Thresholded version of filtered image shown in Fig. 5b.

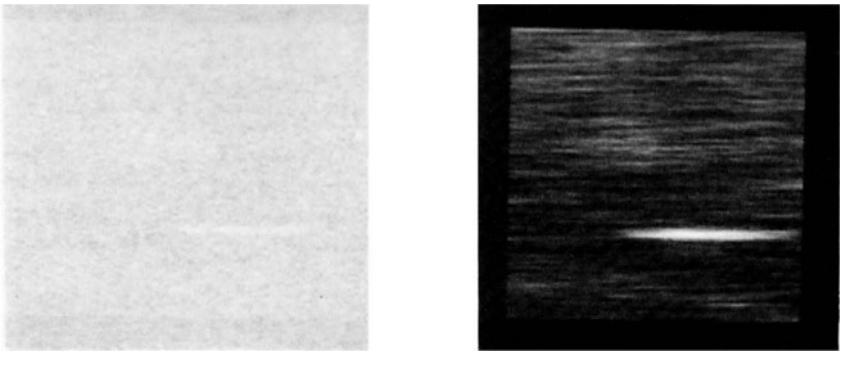

(a) (b)

Figure 7. a) Original radiograph of a crack-like flaw in an aluminum weld (inverted).
b) Filtered result.

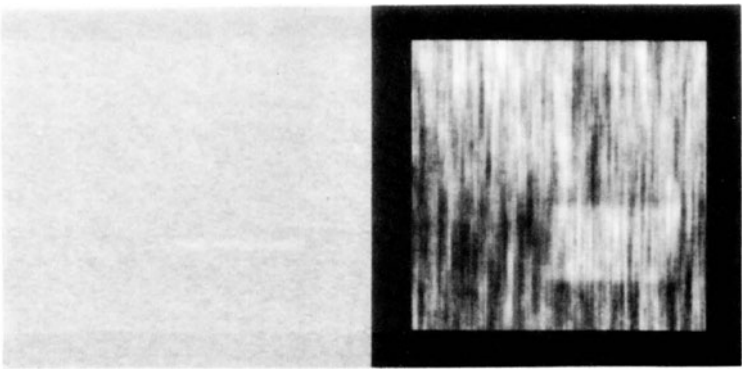

Figure 8. Result of matched filter using orthogonal template.

In order to illustrate the dependence of filter template orientation on flaw detectability when inspecting for crack-like flaws, the matched filter was run using a template orthogonal to that used in Fig. 7b. The resulting image, shown in Figure 8, yields a smeared out feature with little S/N improvement. This filter, if incorporated in a matched filter bank would yield a relatively low output, as expected.

CONCLUSIONS

We have presented several results of matched filtering of high-noise, low-contrast radiographic images that demonstrate the usefulness of this technique. The matched filter is a simple, fast, and easy-to-implement routine for obtaining significant improvement in flaw detectability. We have demonstrated that the filter is quite forgiving in cases where the exact flaw shape and/or noise statistics are unknown. In such cases results are sub-optimal but often useful. Future work will address applications to more complicated part geometries as well as to complicated crack like flaws. In addition, flaw shape distortion and noise texture will be studied.

ACKNOWLEDGEMENT

This work was supported by the Center for Nondestructive Evaluation and the FAA Center for Aviation Systems Reliability at Iowa State University.

REFERENCES

1. D.O. North, "Analysis of the Factors which Determine Signal/Noise Discrimination in Radar", RCA Laboratories, Princeton, N.J. Rept. PTR-6C, June, 1943.
2. S. Chaudhuri, S. Chatterjee, N. Katz, M. Nelson and M. Goldbaum, "Detection of Blood Vessels in Retinal Images Using Two Dimensional Matched Filters", IEEE Transactions on Medical Imaging, Vol. 8, No. 3, 263-269, 1989.
3. W.A.C. Shmidt, "Modified Matched FIlter for Cloud Clutter Suppression", IEEE Transactions on Pattern Analysis and Machine Intelligence, Vol. 12, No. 6, 594-600, 1990.
4. L. O'Gorman and J.V. Nickerson, "Matched Filter Design for Fingerprint Enhancement", IEEE International Conference on Acoustics, Speech and Signal Processing, 916-919, 1988.

5. Detection of Signals in Noise, A.D. Whalen, Academic Press, 1971.
6. Digital Image Processing, 2nd edition, W.K. Pratt, Wiley, 1991.
7. Physics of Industrial Radiology, R. Halmshaw. American Elsevier, 1966.
8. J.N. Gray, "Three Dimensional Modeling of Projection Radiography" in Review of Progress in Quantitative Nondestructive Evaluation, Vol. 7A, D.O. Thompson and D.E. Chimenti, Ed., Plenum Press, 343-348, 1988.
9. J.N. Gray, F. Inanc and B.E. Shull, ""Three Dimensional Modeling of Projection Radiography" in Review of Progress in Quantitative Nondestructive Evaluation, Vol. 8A, D.O. Thompson and D.E. Chimenti, Ed., Plenum Press, 1989.